



Article

Cardiac NF- κ B Acetylation Increases While Nrf2-Related Gene Expression and Mitochondrial Activity Are Impaired during the Progression of Diabetes in UCD-T2DM Rats

Max A. Thorwald ^{1,*} , Jose A. Godoy-Lugo ^{1,2}, Ruben Rodriguez ³, Kimber L. Stanhope ⁴ , James L. Graham ⁴, Peter J. Havel ⁴, Henry Jay Forman ^{1,2} and Rudy M. Ortiz ²

- ¹ Leonard Davis School of Gerontology, University of Southern California, Los Angeles, CA 90017, USA; jgodoy4@ucmerced.edu (J.A.G.-L.); hforman@usc.edu (H.J.F.)
² Department of Molecular and Cell Biology, School of Natural Sciences, University of California, Merced, CA 95343, USA; rortiz@ucmerced.edu
³ Department of Cellular and Molecular Pharmacology, University of California, San Francisco, CA 94143, USA; ruben.rodriguez@ucsf.edu
⁴ Department of Molecular Biosciences, School of Veterinary Medicine and Department of Nutrition, University of California, Davis, CA 95616, USA; klstanhope@ucdavis.edu (K.L.S.); jlgraham@ucdavis.edu (J.L.G.); pjhavel@ucdavis.edu (P.J.H.)
* Correspondence: thorwald@usc.edu; Tel.: +1-213-740-4915



Citation: Thorwald, M.A.; Godoy-Lugo, J.A.; Rodriguez, R.; Stanhope, K.L.; Graham, J.L.; Havel, P.J.; Forman, H.J.; Ortiz, R.M. Cardiac NF- κ B Acetylation Increases While Nrf2-Related Gene Expression and Mitochondrial Activity Are Impaired during the Progression of Diabetes in UCD-T2DM Rats. *Antioxidants* **2022**, *11*, 927. <https://doi.org/10.3390/antiox11050927>

Academic Editors: M.-Saadeh Suleiman and Nicola King

Received: 28 April 2022

Accepted: 3 May 2022

Published: 9 May 2022

Publisher's Note: MDPI stays neutral with regard to jurisdictional claims in published maps and institutional affiliations.



Copyright: © 2022 by the authors. Licensee MDPI, Basel, Switzerland. This article is an open access article distributed under the terms and conditions of the Creative Commons Attribution (CC BY) license (<https://creativecommons.org/licenses/by/4.0/>).

Abstract: The onset of type II diabetes increases the heart's susceptibility to oxidative damage because of the associated inflammation and diminished antioxidant response. Transcription factor NF- κ B initiates inflammation while Nrf2 controls antioxidant defense. Current evidence suggests crosstalk between these transcription factors that may become dysregulated during type II diabetes mellitus (T2DM) manifestation. The objective of this study was to examine the dynamic changes that occur in both transcription factors and target genes during the progression of T2DM in the heart. Novel UC Davis T2DM (UCD-T2DM) rats at the following states were utilized: (1) lean, control Sprague-Dawley (SD; $n = 7$), (2) insulin-resistant pre-diabetic UCD-T2DM (Pre; $n = 9$), (3) 2-week recently diabetic UCD-T2DM (2Wk; $n = 9$), (4) 3-month diabetic UCD-T2DM (3Mo; $n = 14$), and (5) 6-month diabetic UCD-T2DM (6Mo; $n = 9$). NF- κ B acetylation increased 2-fold in 3Mo and 6Mo diabetic animals compared to SD and Pre animals. Nox4 protein increased 4-fold by 6Mo compared to SD. Nrf2 translocation increased 82% in Pre compared to SD but fell 47% in 6Mo animals. GCLM protein fell 35% in 6Mo animals compared to Pre. Hmox1 mRNA decreased 45% in 6Mo animals compared to SD. These data suggest that during the progression of T2DM, NF- κ B related genes increase while Nrf2 genes are suppressed or unchanged, perpetuating inflammation and a lesser ability to handle an oxidant burden altering the heart's redox state. Collectively, these changes likely contribute to the diabetes-associated cardiovascular complications.

Keywords: mitochondrial dysfunction; diabetes; inflammation; antioxidants; oxidative stress

1. Introduction

Type II diabetes (T2DM) is a growing epidemic with more than 70% of its deaths caused by cardiovascular-related complications [1]. Insulin resistance and T2DM have been associated with chronic inflammation and impaired nucleophilic tone [2–4]. Nuclear factor kappa-light-chain-enhancer of activated B cells (NF- κ B) is a transcription factor that primarily regulates inflammatory cascades by increasing cytokine levels to elicit immune responses, many of which directly contribute to increases in oxidant production [5]. Nuclear factor erythroid 2-related factor 2 (Nrf2) primarily regulates genes responsible for neutralizing excess oxidant production, xenobiotic detoxification, and NADPH replenishment [6]. While the mechanisms remain unclear, downstream targets of NF- κ B and Nrf2 have been proposed to regulate each other. This regulation is problematic in diseases associated with

NF- κ B mediated chronic low-grade inflammation and subsequent oxidant generation such as T2DM [7,8].

NF- κ B regulation occurs in the cytosol where it is bound to a family of proteins known as NF- κ B inhibitors (I κ B). I κ B α is phosphorylated allowing NF- κ B p65 to enter the nucleus where it transcribes a battery of genes associated with inflammation and apoptosis [5,9]. Tumor necrosis factor- α (TNF α), a potent inducer and product of NF- κ B stimulation has been implicated in disrupting insulin's action during periods of hyperglycemia [4]. Among other downstream targets associated with NF- κ B gene expression are pro-oxidant enzymes NADPH oxidase 2 (Nox2) and NADPH oxidase 4 (Nox4), both present in cardiac tissue. Nox2 and 4 are both upregulated in the vasculature during the manifestation of T2DM and increase in response to TNF α stimulation [10–12]. Nox proteins produce either superoxide and/or hydrogen peroxide, and their overexpression has been well documented in inducing cardiac hypertrophy and oxidative damage.

Transcription factor Nrf2 is sequestered in the cytosol by kelch-like ECH-associated protein 1 (Keap1) [13] and is liberated after modification of Keap1's cysteines. Nrf2 translocates to the nucleus binding the electrophile response element (EpRE), initiating gene expression [14,15]. Nrf2 increases antioxidant expression in response to a rise in oxidant production; however, during T2DM nuclear Nrf2 translocation and/or antioxidant induction is impaired. Cellular damage accrues each time oxidant levels increase. Degradation of Nrf2 is partially mediated by nuclear glycogen synthase kinase-3 Beta (GSK3 β) through β -TrCP [16–18]. Thus, nuclear Nrf2 import may still be dampened impairing phase II gene responses.

Mitochondria are the largest producers of oxidants [19–21] generating hydrogen peroxide (H₂O₂) and peroxynitrite (ONOO[−]) even under unstressed conditions. H₂O₂ is derived from superoxide (O₂^{·−}) while ONOO[−] is derived from the reaction of nitric oxide (NO) with O₂^{·−}. During T2DM, oxidant production increases from mitochondrial dysfunction [22]. Cardiac mitochondria contain numerous antioxidants including proteins belonging to superoxide dismutase [23], catalase [24], glutathione peroxidase, and transferase families [25]. The latter utilize glutathione (GSH) to mitigate excess oxidant production and detoxify lipid peroxidation products [25]. GSH is produced in the cytosol and imported into the mitochondria for these purposes. However, genes responsible for GSH biosynthesis or utilization are under Nrf2's control and nuclear Nrf2 protein is low during T2DM likely from impaired Nrf2 translocation and/or enhanced degradation. Increases in mitochondrial oxidant production and decreases in antioxidant defense cause damage to accrue increasing mitophagy through localization of parkin to the mitochondria [19,26,27].

NF- κ B and Nrf2 have been studied extensively in numerous diseases including T2DM often with evidence of their crosstalk [7,28–32]. While their crosstalk remains unclear, it is proposed that upon nuclear entry, NF- κ B and Nrf2 compete for CREB which is necessary for either to bind their target sequence of DNA [33]. Conversely, some argue that NF- κ B is required for Nrf2 nuclear import likely through a signaling event caused by prior activation of NF- κ B [34]. Because these transcription factors are often measured independently, we aimed to track their status as T2DM progresses and in a more physiologically relevant but underutilized model of T2DM [35,36]. Here, we show that NF- κ B activation and subsequent target gene expression increases while Nrf2 becomes unresponsive in late T2DM.

2. Methods

All experimental procedures were reviewed and approved by the institutional animal care and use committee of the University of California, Davis (08/07/2008–08/07/2011 IACUC #: 15011).

2.1. Animals

UCD-T2DM rats were generated by crossing obese Sprague-Dawley rats with adult-onset obesity and insulin resistance with ZDF lean rats that have a defect in β -cell/islet function, but were homozygous, wild-type for the leptin receptor [35,37]. The UCD-

T2DM rat has been characterized and validated in more than 20 subsequent peer-reviewed publications [36–38] and closely resembles the pathophysiology of T2DM in humans. T2DM progression was determined by weekly intravenous glucose tolerance as previously described [35]. T2DM manifestation was characterized as having >200mg/dL nonfasting blood glucose for 2 consecutive weeks. Animals in the pre-diabetic group were age matched but did not meet the >200mg/dL criteria for T2DM. Pre animals had elevated fasting plasma insulin compared to SD [35]. Lean Sprague-Dawley (SD; $n = 7$), pre-diabetic UCD-T2DM (Pre; $n = 9$), 2-week diabetic UCD-T2DM (2Wk; $n = 9$), and 3-month diabetic UCD-T2DM (3Mo; $n = 14$) were all 5.5 months of age at the time of tissue collection. The 6-month diabetic UCD-T2DM (6Mo; $n = 9$) rats were approximately 90 days older than all other rats as previously described [37]. Phenotypic data for the animals used in this study has been previously described [35,37] (Table 1). All animals were maintained in a specific pathogen-free facility with a 14 h light, 10 h dark cycle. All animals were given *ad libitum* access to standard laboratory rat chow (Harlan Laboratories, Indianapolis, IN) and water. Prior to dissection, animals were fasted for 13 h and blood was collected via tail vein into EDTA-coated tubes which was used for subsequent assays. Animals were given a 200 mg/kg IP injection of pentobarbital sodium and exsanguinated via cardiac puncture. Heart tissue was snap frozen in liquid nitrogen and stored at $-80\text{ }^{\circ}\text{C}$ [33].

Table 1. Phenotype data for Sprague-Dawley (SD; $n = 7$), pre-diabetic UCD-T2DM (Pre; $n = 9$), 2-week diabetic UCD (2Wk; $n = 9$), 3-month diabetic UCD-T2DM (3Mo; $n = 14$), and 6-month diabetic UCD-T2DM (6Mo; $n = 9$) rats. * Significant difference from SD ($p < 0.05$). † Significant difference from Pre ($p < 0.05$). ‡ Significant difference from 2Wk ($p < 0.05$). § Significant difference from 3Mo ($p < 0.05$).

	SD	Pre	2Wk	3Mo	6Mo
Age (d)	168 ± 1	170 ± 3	168 ± 3	160 ± 2	265 ± 5
Body Mass (g)	404 ± 7	629 ± 5 *	645 ± 18 *	480 ± 13 *, †, ‡	474 ± 13 *, †, ‡
Fasting Glucose (mg/dL)	83 ± 1	96 ± 2 *	98 ± 5 *	189 ± 33 *, †, ‡	384 ± 30 *, †, ‡, §
Non-Fasting Glucose (mg/dL)	112 ± 2	146 ± 8 *	280 ± 30 *, †	508 ± 12 *, †, ‡	592 ± 4 *, †, ‡, §
HbA1c (%)	4.2 ± 0.2	4.1 ± 0.2	5.8 ± 0.4 *, †	12.0 ± 0.7 *, †, ‡	13.6 ± 0.7 *, †, ‡
Fasting Insulin (ng/mL)	0.6 ± 0.1	1.9 ± 0.2 *	2.4 ± 0.3 *	0.9 ± 0.1 †, ‡	0.5 ± 0.1 †, ‡, §

2.2. Western Blot Analyses

A 20 mg piece of frozen mixed ventricle was homogenized in 125 μL of sucrose buffer for subsequent extraction of the mitochondrial, nuclear, and cytosolic fractions [39]. Proteins were assayed as previously described [40] and incubated for 16 h with primary antibodies (diluted 1:100 to 1:4000) against GCLC, GCLM (provided by Dr. Forman), Nox4, Vdac1 (Abcam, Cambridge, MA, USA), NF- κB p65, acetylated-NF- κB (Lys 310), I $\kappa\text{B}\alpha$, p-I $\kappa\text{B}\alpha$, H3, (Cell Signaling, Danvers, MA, USA), Keap1, Nrf2, GSK3 β , Parkin, GAPDH (Santa Cruz Biotechnology, Santa Cruz, CA, USA), 4-hydroxy-2-nonenal (4HNE), Nox2 (EMD Millipore, Burlington, MA, USA), and Hmox1 (Proteintech, Rosemont, IL, USA). Blots were visualized using an Odyssey system (LI-COR Biosciences) and quantified using ImageJ. Nuclear and cytosolic extractions were tested for purity against H3 and GAPDH [39]. Mitochondrial extractions were also tested for purity with Vdac1 and GAPDH. In addition to consistently loading the same amount of total protein per well, values were further normalized by correcting with the densitometry values of Ponceau S staining [41]. Three Western blots were run per protein to include all available biological replicates. All blots contained no less than 2 representative samples per group.

2.3. Real-Time Quantitative PCR Analyses

Total RNA was isolated using TRIzol reagent (Invitrogen, Carlsbad, CA, USA). Genomic DNA was degraded using DNase I enzyme (Roche, Indianapolis, IN, USA). Total RNA purity was confirmed by absorbance at 260/280 and integrity by 1% agarose gel electrophoresis. Complementary DNA was reverse transcribed from genomic DNA-free

RNA (2 µg) using the High-Capacity cDNA Reverse Transcription Kit (Applied Biosystems, Foster City, CA, USA) and oligo-dT. Quantitative PCR reactions were performed in duplicate using an equivalent to 100 ng of RNA and specific primers for Keap1, GSK3β, Nrf2, NF-κB, IκBα, Bach1, GCLM, GCLC, Hmox1, and Nox4 (Table 2). Gene expression was normalized using B2M expression and values were analyzed using the comparative double delta-CT method.

Table 2. Primers and GeneBank accession number for real-time PCR.

Primer Name	Nucleotide Sequence (5'-3')	GeneBank Number
Keap1-F	ATGTGATGAACGGGGCAGTC	NM_057152.2
Keap1-R	AGAACTCCTCCTCCCCGAAG	
Gsk3β-F	CTGGCCACCATCCTTATCCC	NM_032080.1
Gsk3β-R	GAAGCGGCGTTATTGGTCTG	
Nrf2-F	ATTTGTAGATGACCATGAGTCGC	NM_031789.2
Nrf2-R	TGTCCTGCTGTATGCTGCTT	
Bach1-F	CACAAAGTGCAAAGACCCCG	NM_001107113.1
Bach1-R	ATCGCCTGACTGCTCGTATG	
Gclm-F	GTTTCATTGTAGGATCG	NM_017305.2
Gclm-R	GGTGCCTATAGCAACAATCT	
Gclc-F	CTGGACTCATCCCCATTC	NM_012815.2
Gclc-R	GTAGTCAGGATGGTTTGC	
Hmox1-F	GAGCGAAACAAGCAGAACCC	NM_012580.2
Hmox1-R	ACCTCGTGGAGACGCTTTAC	
NF-κB-F	GAGCTGGTGGAGGCCCTG	NM_001276711.1
NF-κB-R	GACAGCGGCGTGGAGAC	
IKBα-F	CTCAAGAAGGAGCGGTTGGT	NM_001105720.2
IKBα-R	CCAAGTGCAGGAACGAGTCT	
Nox4-F	AGATGTTGGGCCTAGGATTGTG	NM_053524.1
Nox4-R	TGTGATCCGCGAAGGTAAGC	
B2m-F	ATGGGAAGCCCAACTTCCTC	NM_012512.2
B2m-R	ATACATCGGTCTCGGTGGGT	

2.4. Biochemical Analyses

Complex I, complex II (Abcam, Cambridge, MA, USA), and TNFα (Meso Scale Discovery, Rockville, MD, USA) assays were measured by ELISA. All samples were analyzed in duplicate and run in a single assay with intra-assay and percent coefficients of variability of less than 10% for all assays.

2.5. Statistics

Means (±SEM) were compared by ANOVA. Means were considered significantly different at $p < 0.05$ using Tukey's HSD. Outliers were removed and replaced with the group mean [42]. Statistical analyses were performed with GraphPad Prism 8 software (Graphpad, San Diego, CA, USA).

3. Results

3.1. Body Mass, Glucose, and Insulin Measurements

Phenotype data was collected to track the progression of T2DM. Body mass was increased in Pre (56%) and 2Wk (60%) animals compared to SD. Body mass was 26% lower in 3Mo remained lower in 6Mo animals compared to SD. Fasting blood glucose increased 16% in Pre and 2Wk animals compared to SD. Fasting blood glucose further increased 129% in 3Mo and 3.5-fold in 6Mo old animals, respectively. Non-fasting blood glucose was 30% higher in Pre animals compared to SD. Non-fasting blood glucose further increased in 2Wk (1.5-fold), 3Mo (3.5-fold), and 6Mo (4-fold) animals compared to SD. Glycated hemoglobin (HbA1c) increased 4-fold in 2Wk animals compared to SD. HbA1c levels further increased 3-fold in 3Mo and 6Mo animals. Insulin levels were 2-fold higher in

pre-diabetic and 3-fold in 2-week diabetic animals. Insulin levels were reduced 63% in 3Mo and 80% in 6Mo animals compared to 2Wk animals (Table 1).

3.2. Cardiac NF- κ B Signaling Is Increased in UCD-T2DM Rats as Diabetes Progresses

Chronic inflammation is synonymous with T2DM. Canonical components of NF- κ B signaling were measured to determine if similar outcomes occurred in UCD-T2DM rats. NF- κ B transcripts increased 2.5-fold in Pre compared to SD and remained elevated in 2Wk and 3Mo groups (Figure 1A). No changes were observed in cytosolic NF- κ B expression (Figure 1B). Nuclear NF- κ B increased in 2Wk (43%) and 3Mo (71%) animals compared to Pre. Nuclear NF- κ B decreased 37% in 6Mo animals compared to 3Mo (Figure 1C). No differences were observed in NF- κ B translocation (not shown). Acetylation of Lys310 on Nuclear NF- κ B protein increased 2-fold in 3Mo and 6Mo animals compared to SD and Pre (Figure 1D). I κ B α transcripts increased in 2- and 3-fold in 3Mo and 6Mo animals compared to SD, respectively. 6Mo animals also had 2-fold more I κ B α transcripts than Pre (Figure 1E). No changes were observed in the ratio of phosphorylated and native I κ B α protein (Figure 1F). Overall, these data suggest that as diabetes progresses, cardiac NF- κ B activation increases.

3.3. NF- κ B Associated Inflammatory Genes Increase as T2DM Progresses

Several downstream targets responsible for heightened inflammation and oxidant production were measured to determine the increase in NF- κ B activation altered gene expression. Plasma TNF α levels increased 112% in 3Mo and 134% in 6Mo animals compared to SD (Figure 2A). Nox2 protein increased 82% in Pre animals compared to SD and increased further by 134% in 6Mo animals (Figure 2B). Nox4 transcripts increased 4-fold in Pre, 2Wk, and 3Mo animals compared to SD (Figure 2C). Nox4 expression increased 2-, 3-, and 4-fold in 2Wk, 3Mo, and 6Mo old animals compared to SD, respectively. Nox4 expression was increased 77% and 83% in 6Mo animals compared to Pre and 2Wk, respectively (Figure 2D).

3.4. Nrf2 Signaling Is Impaired or Unresponsive in UCD-T2DM Hearts

Nrf2 is the master regulator of antioxidant gene production and was measured to ascertain its status during T2DM progression. Nrf2 transcripts were unchanged except in 6Mo animals where they were 2- and 4-fold higher than 2Wk and 3Mo animals, respectively (Figure 3A). Cytosolic Nrf2 decreased 54% in Pre and 33% 2Wk animals compared to SD, respectively. Cytosolic Nrf2 levels returned to baseline at 6Mo (Figure 3B). Nuclear Nrf2 was decreased 15% in Pre and 25% in 2Wk animals compared to SD. The 6Mo animals returned to baseline (Figure 3C). Nrf2 translocation increased 82% in Pre compared to SD. Nrf2 translocation was decreased in 2Wk (−60%) and 6Mo (−47%) animals compared to Pre (Figure 3D). Keap1 transcripts increased 78% in Pre compared to SD and remained elevated in 2Wk (+90%) and 3Mo (+63%) groups. Transcripts in 6Mo animals returned to baseline (Figure 3E). Keap1 expression decreased 33% in 6Mo animals compared to Pre (Figure 3F). GSK3 β transcripts increased 2-fold in Pre animals compared to SD and remained elevated in 2Wk, 3Mo, and 6Mo old animals (Figure 3G). Nuclear GSK3 β expression increased by 23% in 6Mo animals compared to SD (Figure 3H). Bach1 transcripts were unchanged except in the 6Mo animals where they increased 3.5-fold compared to the SD, 2Wk, and 3Mo groups (Figure 3I). These results demonstrate that Nrf2 signaling is impacted negatively during the progression of T2DM.

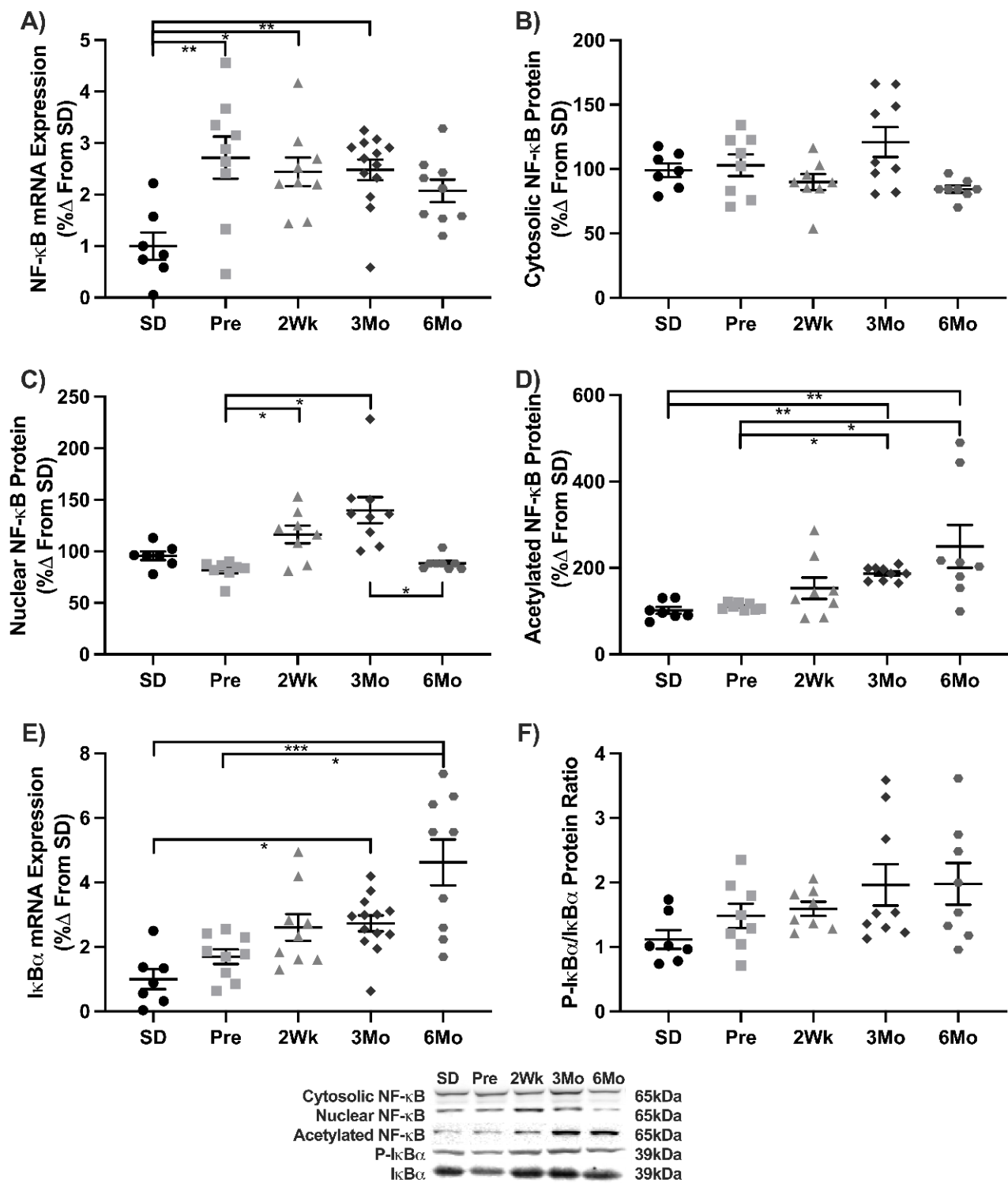


Figure 1. NF-κB signaling during the progression of T2DM. Mean ± SEM values of (A) NF-κB mRNA, (B) cytosolic NF-κB protein, (C) nuclear NF-κB protein, (D) acetylated Lys310 nuclear NF-κB protein, (E), IκBα mRNA, and (F) the ratio of phosphorylated to native IκBα protein in Sprague-Dawley (SD; *n* = 7), pre-diabetic UCD-T2DM (Pre; *n* = 9), 2-week diabetic UCD (2Wk; *n* = 9), 3-month diabetic UCD-T2DM (3Mo; *n* = 13), and 6-month diabetic UCD-T2DM (6Mo; *n* = 9) rats. * *p* < 0.05, ** *p* < 0.01, *** *p* < 0.001.

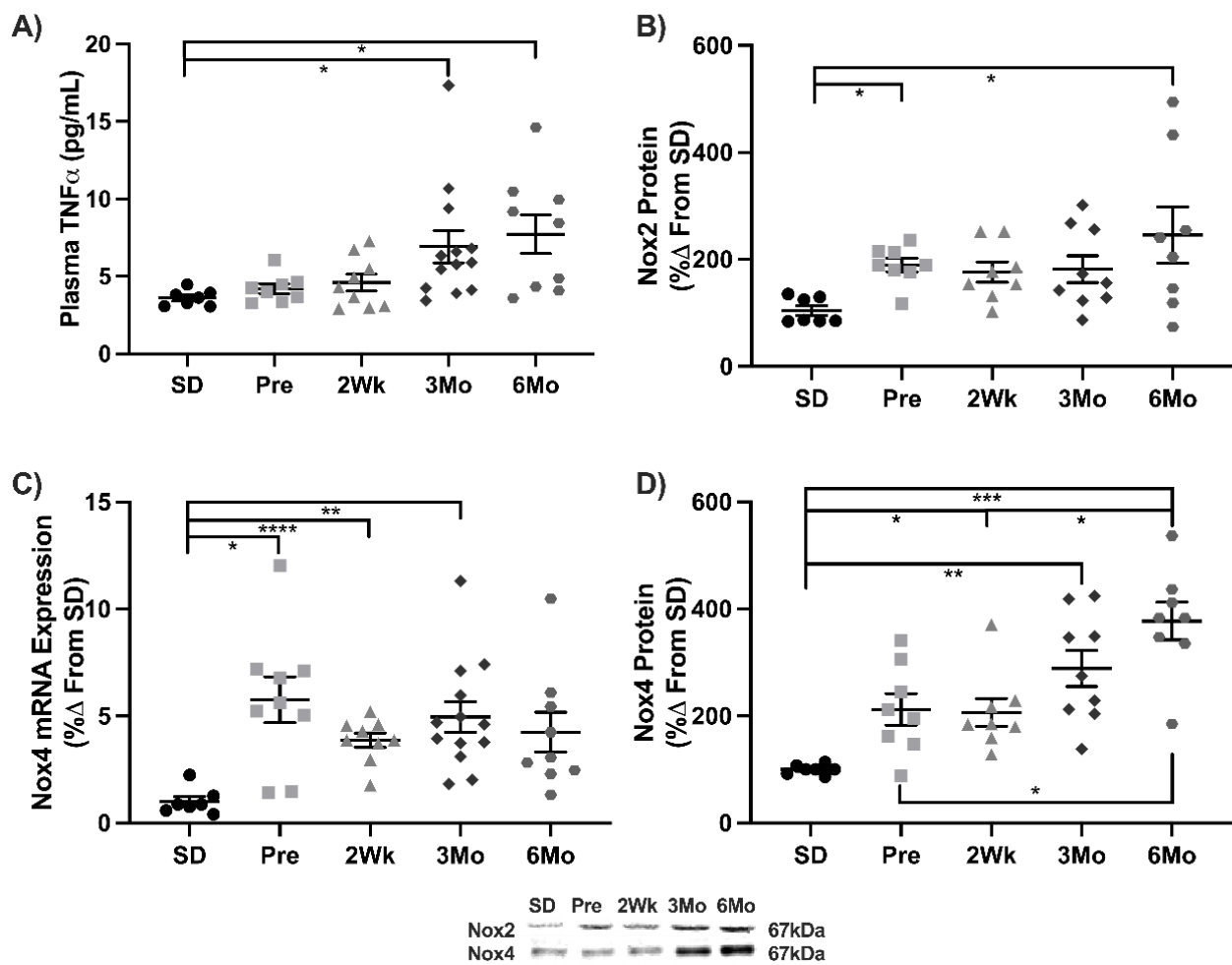


Figure 2. Downstream targets of NF- κ B activation. Mean \pm SEM values of (A) plasma TNF α , (B) Nox2 protein, (C) Nox4 mRNA, and (D) Nox4 protein in Sprague-Dawley (SD; $n = 7$), pre-diabetic UCD-T2DM (Pre; $n = 9$), 2-week diabetic UCD (2Wk; $n = 9$), 3-month diabetic UCD-T2DM (3Mo; $n = 13$), and 6-month diabetic UCD-T2DM (6Mo; $n = 9$) rats. * $p < 0.05$, ** $p < 0.01$, *** $p < 0.001$, **** $p < 0.0001$.

3.5. Nrf2 Related Genes Are Unaltered or Reduced as T2DM Progresses

GCLC transcripts increased in Pre animals 42% compared to SD. GCLC transcripts decreased in 2Wk (−46%), 3Mo (−30), and 6Mo (−60%) animals compared to Pre. The 6Mo animals had the lowest number of transcripts with a 43% reduction compared to SD and 3Mo animals (Figure 4A). No changes were observed in GCLC protein (Figure 4B) or GCLM transcripts (Figure 4C). GCLM expression was decreased 35% in 6Mo animals compared to Pre and 2Wk animals (Figure 4D). Hmox1 transcripts decreased 45% in 6Mo animals compared to SD (Figure 4E). Hmox1 protein increased 67% in 3Mo (Figure 4F). These results suggest that reductions in Nrf2-related genes in concert with heightened NF- κ B genes may make the heart more susceptible to oxidative damage.

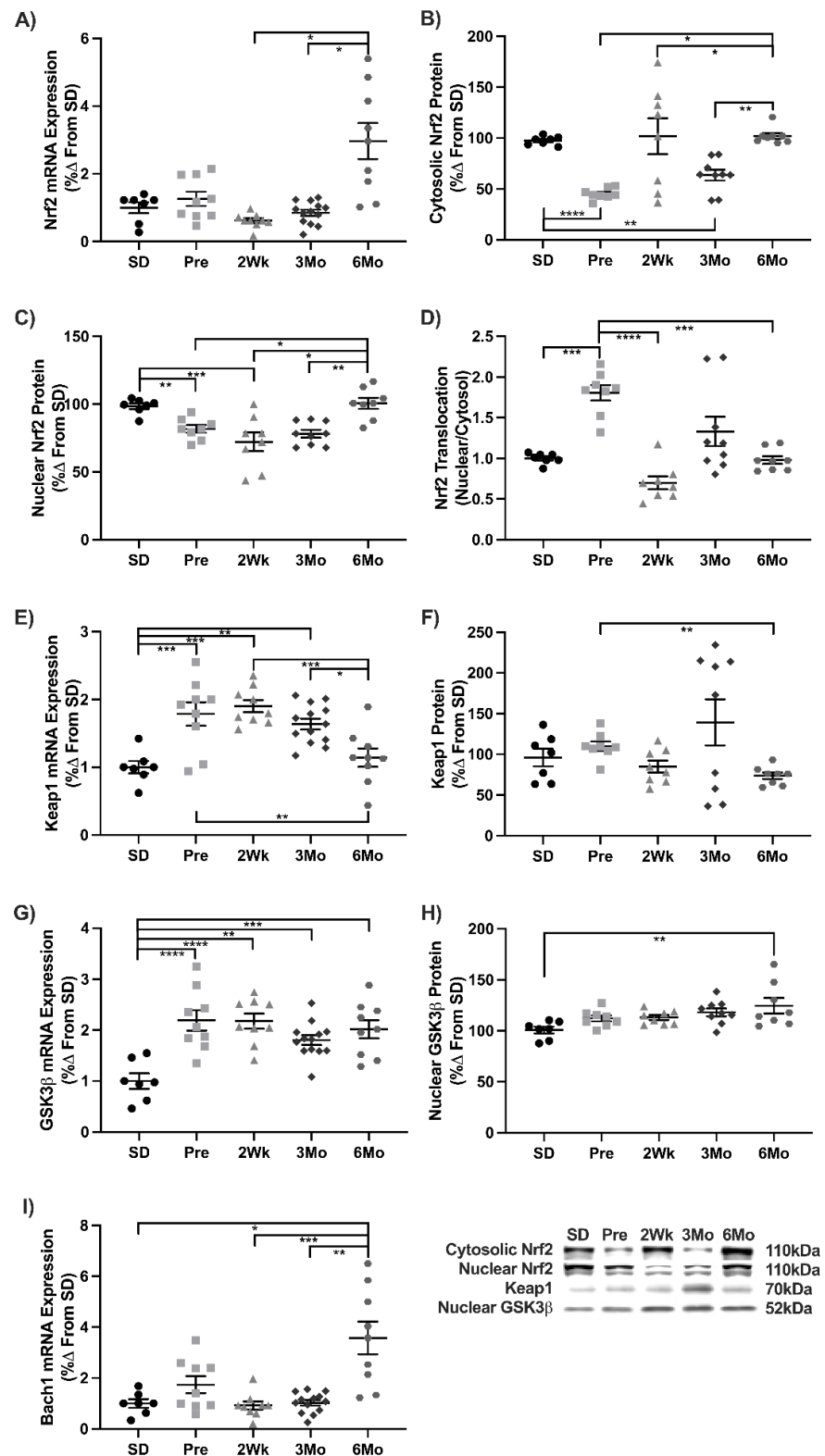


Figure 3. Nrf2 signaling during the progression of T2DM. Mean ± SEM values of (A) Nrf2 mRNA, (B) cytosolic Nrf2 protein, (C) nuclear Nrf2 protein, (D) Nrf2 translocation, (E) Keap1 mRNA, (F) Keap1 protein, (G) GSK3β mRNA, (H) nuclear GSK3β protein, and (I) Bach1 mRNA in Sprague-Dawley (SD; *n* = 7), pre-diabetic UCD-T2DM (Pre; *n* = 9), 2-week diabetic UCD (2Wk; *n* = 9), 3-month diabetic UCD-T2DM (3Mo; *n* = 13), and 6-month diabetic UCD-T2DM (6Mo; *n* = 9) rats. * *p* < 0.05, ** *p* < 0.01, *** *p* < 0.001, **** *p* < 0.0001.

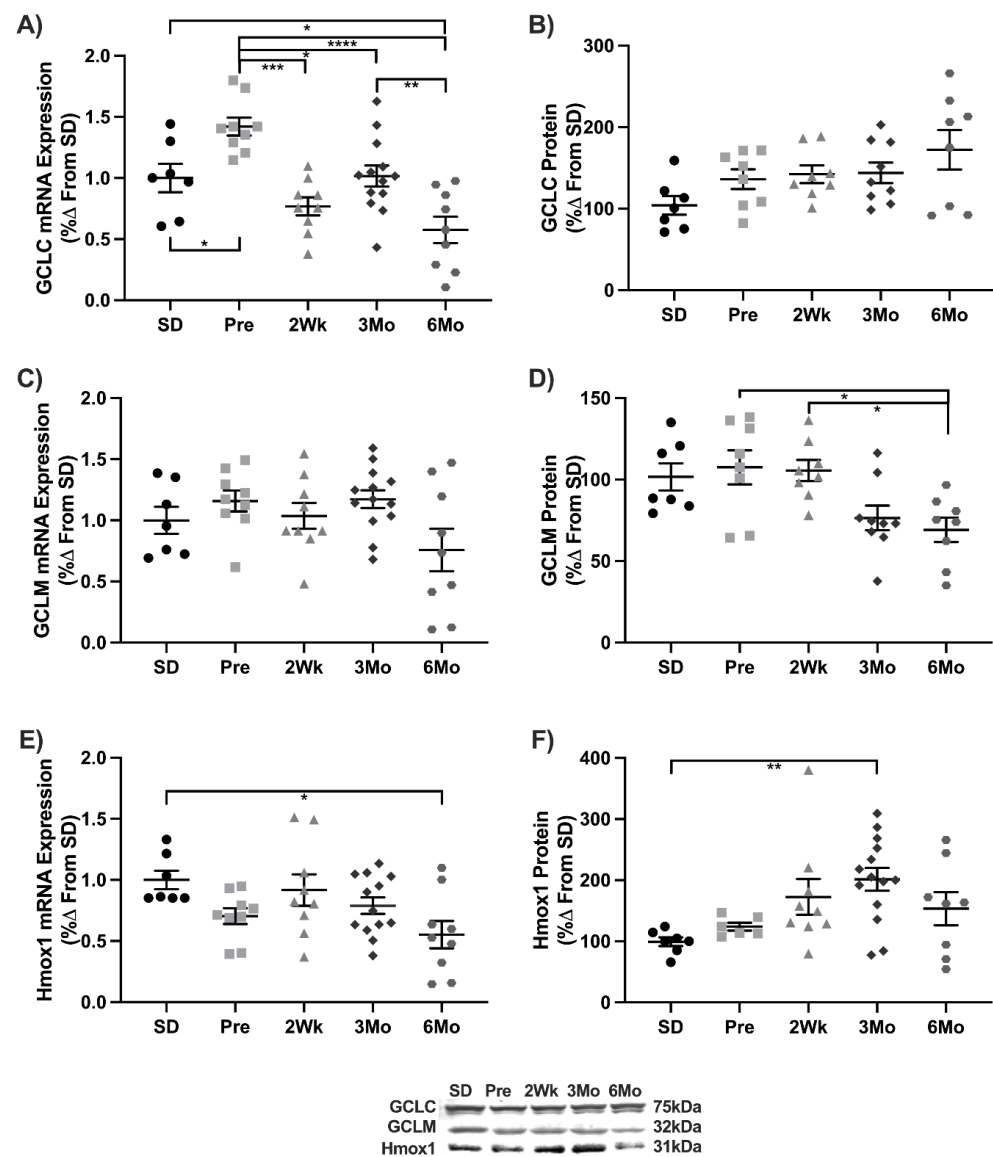


Figure 4. Downstream targets of cardiac Nrf2 activation are decreased or unchanged six months after the onset of T2DM. Mean \pm SEM values of (A) GCLC mRNA, (B) GCLC protein, (C) GCLM mRNA, (D) GCLM protein, (E) Hmox1 mRNA, and (F) Hmox1 protein in Sprague-Dawley (SD; $n = 7$), pre-diabetic UCD-T2DM (Pre; $n = 9$), 2-week diabetic UCD (2Wk; $n = 9$), 3-month diabetic UCD-T2DM (3Mo; $n = 14$), and 6-month diabetic UCD-T2DM (6Mo; $n = 9$) rats. * $p < 0.05$, ** $p < 0.01$, *** $p < 0.001$, **** $p < 0.0001$.

3.6. UCD-T2DM Rats Have Mitochondrial Dysfunction and Increased Mitochondrial Damage Consistent with T2DM Pathology

Mitochondrial function and damage were measured to determine if the mitochondrial dysfunction present in T2DM and other animals was observed in UCD-T2DM rats. Mitochondrial complex I activity decreased 47% in the 2Wk old ventricle compared to SD and remained suppressed in 3Mo animals by 51% (Figure 5A). Complex II was lowered in the Pre animals 50% compared to SD. Development of T2DM further decreased complex II activity in 2Wk old animals compared to SD at 62% and remained suppressed in 3Mo (−64%) and 6Mo (−67%) animals (Figure 5B). Mitochondrial HNE content was measured to determine the oxidative damage accrued in the mitochondria. HNE levels increased at 73% in 3Mo and remained elevated in 6Mo (+37%) old animals (Figure 5C). Mitochondrial parkin increased in the mitochondrial fraction 60% in the Pre animals compared to SD. This

increase was sustained in the 3Mo (+74%) and 6Mo (+56%) animals (Figure 5D). The ratio of native and Phosphorylated AMPK (Thr172) demonstrated a reduction in Pre animals by 32%. These reductions were observed in 2Wk (−43%) and 6Mo (−47%) animals as well (Figure 5E). Collectively, these decreases in mitochondrial complex activity and increases in HNE and parkin suggest cardiac mitochondrial dysfunction in the UCD-T2DM rats consistent with T2DM pathogenesis.

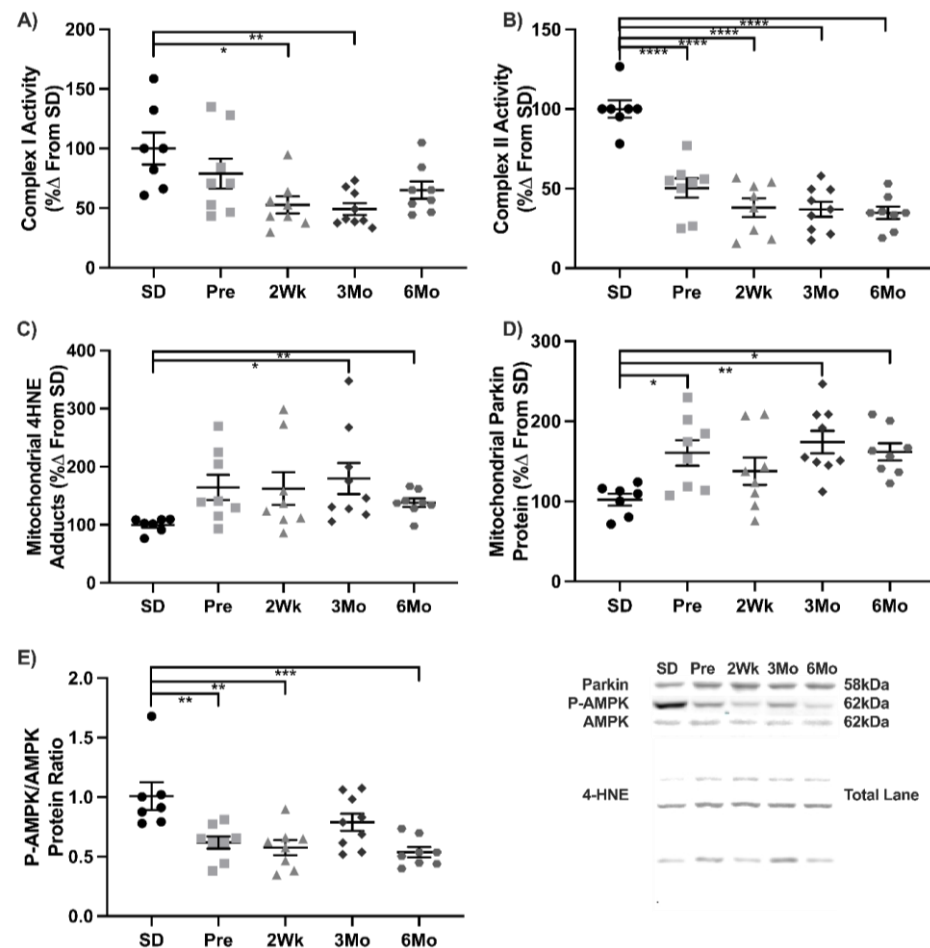


Figure 5. Mitochondria dysfunction and oxidative damage increase as T2DM progresses. Mean \pm SEM values of (A) Complex I activity, (B) Complex II activity, (C) mitochondrial 4HNE adducts, (D) mitochondrial Parkin protein, and (E) ratio of phosphorylated (T172) to native AMPK protein in Sprague-Dawley (SD; $n = 7$), pre-diabetic UCD-T2DM (Pre; $n = 9$), 2-week diabetic UCD (2Wk; $n = 9$), 3-month diabetic UCD-T2DM (3Mo; $n = 13$), and 6-month diabetic UCD-T2DM (6Mo; $n = 9$) rats. * $p < 0.05$, ** $p < 0.01$, *** $p < 0.001$, **** $p < 0.0001$.

4. Discussion

Chronic low-grade inflammation during T2DM and obesity are established characteristics due to activation of NF- κ B. While the stimulation of inflammatory cascades and suppression of antioxidants systems are well documented in T2DM, here we provide data demonstrating the temporal enhancement of cardiac NF- κ B associated with increases in acetylation and Nox proteins, and diminished activation of Nrf2 with the transition from insulin resistance to T2DM.

NF- κ B is tethered in the cytosol by I κ B α , which requires phosphorylation to liberate NF- κ B and allow for its nuclear import. Despite an increase in I κ B α mRNA during the progression of T2DM, this increase did not translate to a detectable increase in I κ B α phosphorylation. NF- κ B mRNA increased in the prediabetic animals and remained elevated but did not result in an increase in cytosolic NF- κ B protein suggesting that either the

increase in mRNA expression was not sufficient to maintain elevated protein levels or NF- κ B turnover increased as T2DM progressed. However, nuclear NF- κ B p65 increased as T2DM progressed except in the 6-month diabetic hearts where NF- κ B levels were the same as the control animals suggesting that the lack of a decrease in the cytosol was a factor of nuclear accumulation. Despite the lack of nuclear NF- κ B in the insulin-resistant and late-stage diabetic animals, acetylation of nuclear NF- κ B at Lys310 rose sharply with the progression of T2DM. This suggests acetylation of NF- κ B may be more relevant for assessing NF- κ B activation rather than nuclear NF- κ B protein. While acetylated lysine 310 bears no consequence on DNA binding, it is essential for full transcriptional activity of NF- κ B p65 illustrating increased activation during disease progression [43,44].

Downstream targets of NF- κ B were measured to determine if increased p65 acetylation translated into increased target genes. Plasma TNF α levels matched changes in NF- κ B activation. TNF α is a potent inducer of oxidant production through the Nox family, which directly contributes to oxidant generation through use of NADPH [5,11,45]. Nox2 and Nox4 are the predominantly expressed isoforms in the cardiovascular system with Nox4 regulated primarily by mRNA copy number [46]. Nox expression increased in the insulin-resistant animals preceding nuclear NF- κ B increases suggesting their assemblage may occur before the onset of chronic inflammation. Increases in the Nox family during insulin resistance has been largely attributed to the renin–angiotensin system stimulation in other diabetic models [47]. NF- κ B acetylation paralleled the increase in plasma TNF α levels and Nox proteins in 3- and 6-month hearts suggesting that acetylation and TNF α may both enhance Nox expression in late T2DM. These increases are characteristic of the chronic, systemic inflammation associated with oxidant generation during the manifestation of T2DM [48].

Meanwhile Nrf2, which is responsible for initiating transcription of genes involved in mitigating excess oxidant production NADPH, decreased or was unchanged during T2DM progression. Nuclear Nrf2 accumulation does not occur without modification of inhibitory cytosolic protein Keap1. Keap1 transcripts increased in the insulin-resistant hearts and remained elevated until 6-month diabetic state. Keap1 protein matched mRNA and was also lowered at 6 months. Nrf2 translocation increased in the insulin resistant animals but decreased in the 2-week and 6-month diabetic hearts suggesting that Nrf2 is functional during insulin resistance but becomes dysregulated shortly after the onset of T2DM. While the levels of Nrf2 mRNA, and cytosolic and nuclear protein content increased in the 6-month diabetic hearts, nuclear Nrf2 inhibition may impair activation during late T2DM. GSK3 β has been proposed to facilitate degradation of nuclear Nrf2 [16]. Nuclear GSK3 β increased in late-stage T2DM potentially stifling Nrf2 activation. Bach1, a known competitor of EpRE binding [49,50], was unchanged during the diabetes progression; however, in 6-month diabetic hearts, Bach1 transcripts increased suggesting that nuclear Nrf2's potential to bind to the EpRE and initiate transcription of target genes during advanced diabetes may be inhibited by competition of Bach1. Collectively, these data demonstrate that despite the increase in Nrf2 mRNA and relatively unaltered protein levels by 6 months, increases in nuclear regulators GSK3 β and Bach1 likely limit Nrf2 activation.

To determine if the absence of Nrf2 translocation impacted its target genes, we measured two critical enzymes for the GSH cycle. GSH is the most abundant, non-enzymatic antioxidant whose production is altered in diabetic hearts [51]. During cellular stress, GSH increases to counter the increases in oxidants. Glutamate cysteine ligase catalytic subunit (GCLC) and glutamate cysteine ligase modifier subunit (GCLM) dimerize to produce glutathione cysteine ligase (GCL). GCLC catalyzes the production of gamma-glutamylcysteine while GCLM increases the activity of GCLC greatly [52] and therefore is the rate limiting subunit for GSH synthesis. GCLC increased in the insulin resistant hearts but decreased following the onset of diabetes. No changes were observed in GCLC protein; however, GCLM protein decreased in the 6-month hearts. GCLM reductions suggest GSH biosynthesis is impaired 6 months after the onset of diabetes. Heme oxygenase 1 (Hmox1), another Nrf2 target gene involved in heme metabolism produces anti-inflammatory byproduct carbon

monoxide (CO) which is known to negatively regulate NF- κ B target genes [7,53]. Hmox1 mRNA was decreased; however, protein levels were increased by 3 months but were not different at 6 months, consistent with our other findings. Downregulation of Hmox1 mRNA and lack of response in Hmox1 protein at 6 months provides further evidence of the impaired Nrf2 activity. Blunted Nrf2 translocation further suggests that heightened NF- κ B-mediated inflammation may impair Nrf2 activity and subsequent antioxidant defense during the progression of T2DM.

Energy balance is essential to antioxidant function where NADPH is required for many redox reactions [54]. Mitochondrial dysfunction is a hallmark of T2DM and was measured to assess the severity of the mitochondrial dysfunction in relation to the simultaneous changes in NF- κ B and Nrf2 associated with the progression of T2DM [22]. Complex I and complex II decreased as diabetes progressed suggesting that the mitochondrial electron transport is impaired during the progression of T2DM. Dysfunction in the electron transport chain has been linked to increased oxidant production [55]. Parkin accumulates on the outside of damaged mitochondria inducing mitophagy [26,27]. The early and sustained increase in parkin suggests that the progression of T2DM was associated damaged mitochondria increasing the potential for mitophagy and altered mitochondrial function. Additionally, mitochondrial 4-HNE adducts, a consequence of lipid peroxidation, increased in late stage T2DM animals providing further evidence of the increase in mitochondrial damage. 4-HNE during the initiation of insulin resistance is consistent with other T2DM models [40]. AMPK acts as an energy sensor where phosphorylation of AMPK increases uptake of glucose and fatty acids. In as early as the pre-diabetic state, the ratio of phosphorylated to native AMPK decreased suggesting that cellular energetics were disrupted as a likely consequence of insulin resistance. These data suggest that cardiac mitochondria progressively worsen with the development of T2DM, paralleling the increased acetylation of NF- κ B and impairment in Nrf2. Reductions in energy production and Nrf2-related antioxidants would increase the susceptibility of oxidative damage in the diabetic heart.

These findings simultaneously track temporal alterations in two key transcription factors involved in T2DM and highlight that increased NF- κ B and blunted Nrf2-mediated antioxidant responses are key contributors to T2DM. Furthermore, increased acetylation of NF- κ B was associated with increased plasma TNF α and Nox protein expression, likely contributing to an increase in oxidant production in the diabetic heart while antioxidant defense and mitochondrial function decrease. These differences in the activation of NF- κ B and Nrf2 that manifest in the prediabetic state and worsen through disease progression impart a heavy burden on the cardiovascular system, leading to increased oxidative damage.

5. Conclusions

We highlight crosstalk between cardiac NF- κ B and Nrf2 during progression of T2DM suggesting that impairment of Nrf2 is not only through lack of nuclear translocation but potentially through simultaneous activation of NF- κ B. Most changes occur within 2 weeks of T2DM onset and are further exacerbated by 3 months and sustained by 6 months suggesting a permanent transition. Alterations in these key transcription factors illustrate the importance of mitigating chronic inflammation and bolstering antioxidant responses during early onset insulin resistance before it progresses to a frank T2DM condition.

Author Contributions: Conceptualization, M.A.T., P.J.H., H.J.F. and R.M.O.; methodology, J.L.G., K.L.S. and P.J.H.; validation, M.A.T. and J.L.G.; formal analysis, M.A.T., J.A.G.-L. and J.L.G.; investigation, M.A.T., J.A.G.-L. and J.L.G.; resources, J.L.G., K.L.S. and P.J.H.; data curation, M.A.T., J.A.G.-L. and J.L.G.; writing—original draft preparation, M.A.T., J.A.G.-L., J.L.G., P.J.H., H.J.F. and R.M.O.; writing—review and editing, M.A.T., J.A.G.-L., R.R., J.L.G., K.L.S., P.J.H., H.J.F. and R.M.O.; visualization, M.A.T., P.J.H., H.J.F. and R.M.O.; supervision, H.J.F. and R.M.O.; project administration, P.J.H., R.M.O.; funding acquisition, P.J.H. and R.M.O. All authors have read and agreed to the published version of the manuscript.

Funding: M. Thorwald: J. Godoy-Lugo, R. Rodriguez, were supported by internal funding from University of California Merced. J. Godoy-Lugo was supported by the UC-MEXUS Consejo Nacional

de Ciencia y Tecnologia (CONACYT) fellowship. P.J. Havel's laboratory received funding during the project period from NIH grants R01HL-091333, R01HL-107256, R01HL-121324, U24DK-092993, RC1DK-087307 and R01DK-095060 and a Multicampus Award from the University of California, Office of the President (Award #142691).

Institutional Review Board Statement: The animal study protocol was approved by the Institutional Review Board of the University of California, Davis (#15011, 08/07/2008–08/07/2011).

Informed Consent Statement: Not applicable.

Data Availability Statement: Data is contained within the article.

Acknowledgments: The authors would like to thank our colleagues for their thorough review of the manuscript drafts.

Conflicts of Interest: The authors declare no conflict of interest.

Ethics Approval and Consent to Participate: All experimental procedures were reviewed and approved by the institutional animal care and use committee of the University of California, Davis.

References

1. Laakso, M. Cardiovascular disease in type 2 diabetes from population to man to Mechanisms. *Diabetes Care* **2010**, *33*, 442–449. [[CrossRef](#)] [[PubMed](#)]
2. Velmurugan, G.V.; Sundaresan, N.R.; Gupta, M.P.; White, C. Defective Nrf2-dependent redox signalling contributes to microvascular dysfunction in type 2 diabetes. *Cardiovasc. Res.* **2013**, *100*, 143–150. [[CrossRef](#)] [[PubMed](#)]
3. Cheng, X.; Siow, R.C.; Mann, G.E. Impaired redox signaling and antioxidant gene expression in endothelial cells in diabetes: A role for mitochondria and the nuclear factor- κ B-related factor 2-kelch-like ECH-associated protein 1 defense pathway. *Antioxid. Redox Signal.* **2011**, *14*, 469–487. [[CrossRef](#)] [[PubMed](#)]
4. Hotamisligil, G.S.; Shargill, N.S.; Spiegelman, B.M. Adipose expression of tumor necrosis factor- α : Direct role in obesity-linked insulin resistance. *Science* **1993**, *259*, 87–91. [[CrossRef](#)]
5. Hayden, M.S.; Ghosh, S. NF- κ B, the first quarter-century: Remarkable progress and outstanding questions. *Genes Dev.* **2012**, *26*, 203–234. [[CrossRef](#)]
6. Jaramillo, M.C.; Zhang, D.D. The emerging role of the Nrf2–Keap1 signaling pathway in cancer. *Genes Dev.* **2013**, *27*, 2179–2191. [[CrossRef](#)]
7. Wardyn, J.D.; Ponsford, A.H.; Sanderson, C.M. Dissecting molecular cross-talk between Nrf2 and NF- κ B response pathways. *Biochem. Soc. Trans.* **2015**, *43*, 621–626. [[CrossRef](#)]
8. Soares, M.P.; Seldon, M.P.; Gregoire, I.P.; Vassilevskaia, T.; Berberat, P.O.; Yu, J.; Tsui, T.-Y.; Bach, F.H. Heme oxygenase-1 modulates the expression of adhesion molecules associated with endothelial cell activation. *J. Immunol.* **2004**, *172*, 3553–3563. [[CrossRef](#)]
9. Brown, K.; Gerstberger, S.; Carlson, L.; Franzoso, G.; Siebenlist, U. Control of I kappa B-alpha proteolysis by site-specific, signal-induced phosphorylation. *Science* **1995**, *267*, 1485–1488. [[CrossRef](#)]
10. Manea, S.-A.; Constantin, A.; Manda, G.; Sasson, S.; Manea, A. Regulation of Nox enzymes expression in vascular pathophysiology: Focusing on transcription factors and epigenetic mechanisms. *Redox Biol.* **2015**, *5*, 358–366. [[CrossRef](#)]
11. Manea, A.; Tanase, L.I.; Raicu, M.; Simionescu, M. Transcriptional regulation of NADPH oxidase isoforms, Nox1 and Nox4, by nuclear factor- κ B in human aortic smooth muscle cells. *Biochem. Biophys. Res. Commun.* **2010**, *396*, 901–907. [[CrossRef](#)] [[PubMed](#)]
12. Kuroda, J.; Ago, T.; Matsushima, S.; Zhai, P.; Schneider, M.D.; Sadoshima, J. NADPH oxidase 4 (Nox4) is a major source of oxidative stress in the failing heart. *Proc. Natl. Acad. Sci. USA* **2010**, *107*, 15565–15570. [[CrossRef](#)] [[PubMed](#)]
13. Itoh, K.; Ye, P.; Matsumiya, T.; Tanji, K.; Ozaki, T. Emerging functional cross-talk between the Keap1-Nrf2 system and mitochondria. *J. Clin. Biochem. Nutr.* **2015**, *56*, 91–97. [[CrossRef](#)]
14. Sasaki, H.; Sato, H.; Kuriyama-Matsumura, K.; Sato, K.; Maehara, K.; Wang, H.; Tamba, M.; Itoh, K.; Yamamoto, M.; Bannai, S. Electrophile response element-mediated induction of the cystine/glutamate exchange transporter gene expression. *J. Biol. Chem.* **2002**, *277*, 44765–44771. [[CrossRef](#)]
15. Kannan, M.B.; Solovieva, V.; Blank, V. The small MAF transcription factors MAFF, MAFG and MAFK: Current knowledge and perspectives. *Biochim. Biophys. Acta* **2012**, *1823*, 1841–1846. [[CrossRef](#)]
16. Rada, P.; Rojo, A.I.; Chowdhry, S.; McMahan, M.; Hayes, J.D.; Cuadrado, A. SCF/ β -TrCP promotes glycogen synthase kinase 3-dependent degradation of the Nrf2 transcription factor in a keap1-independent manner. *Mol. Cell. Biol.* **2011**, *31*, 1121–1133. [[CrossRef](#)] [[PubMed](#)]
17. Hayes, J.D.; Chowdhry, S.; Dinkova-Kostova, A.T.; Sutherland, C. Dual regulation of transcription factor Nrf2 by Keap1 and by the combined actions of β -TrCP and GSK-3. *Biochem. Soc. Trans.* **2015**, *43*, 611–620. [[CrossRef](#)]
18. Chowdhry, S.; Zhang, Y.; McMahan, M.; Sutherland, C.; Cuadrado, A.; Hayes, J.D. Nrf2 is controlled by two distinct β -TrCP recognition motifs in its Neh6 domain, one of which can be modulated by GSK-3 activity. *Oncogene* **2012**, *32*, 3765–3781. [[CrossRef](#)]
19. Van Remmen, H.; Richardson, A. Oxidative damage to mitochondria and aging. *Exp. Gerontol.* **2001**, *36*, 957–968. [[CrossRef](#)]

20. Newsholme, P.; Haber, E.P.; Hirabara, S.M.; Rebelato, E.L.O.; Procopio, J.; Morgan, D.; Oliveira-Emilio, H.C.; Carpinelli, A.; Curi, R. Diabetes associated cell stress and dysfunction: Role of mitochondrial and non-mitochondrial ROS production and activity. *J. Physiol.* **2007**, *583*, 9–24. [[CrossRef](#)]
21. Korshunov, S.S.; Skulachev, V.P.; Starkov, A.A. High protonic potential actuates a mechanism of production of reactive oxygen species in mitochondria. *FEBS Lett.* **1997**, *416*, 15–18. [[CrossRef](#)]
22. Belosludtsev, K.N.; Belosludtseva, N.V.; Dubinin, M.V. Diabetes mellitus, mitochondrial dysfunction and Ca²⁺-dependent permeability transition pore. *Int. J. Mol. Sci.* **2020**, *21*, 6559. [[CrossRef](#)] [[PubMed](#)]
23. Shen, X.; Zheng, S.; Metreveli, N.S.; Epstein, P.N. Protection of cardiac mitochondria by overexpression of MnSOD reduces diabetic cardiomyopathy. *Diabetes* **2006**, *55*, 798–805. [[CrossRef](#)] [[PubMed](#)]
24. Radi, R.; Turrens, J.; Chang, L.; Bush, K.; Crapo, J.; Freeman, B. Detection of catalase in rat heart mitochondria. *J. Biol. Chem.* **1991**, *266*, 22028–22034. [[CrossRef](#)]
25. Mari, M.; De Gregorio, E.; De Dios, C.; Roca-Agujetas, V.; Cucarull, B.; Tutusaus, A.; Morales, A.; Colell, A. Mitochondrial glutathione: Recent insights and role in disease. *Antioxidants* **2020**, *9*, 909. [[CrossRef](#)] [[PubMed](#)]
26. Pickrell, A.M.; Youle, R.J. The roles of PINK1, parkin, and mitochondrial fidelity in parkinson's disease. *Neuron* **2015**, *85*, 257–273. [[CrossRef](#)]
27. Zheng, X.; Hunter, T. Parkin mitochondrial translocation is achieved through a novel catalytic activity coupled mechanism. *Cell Res.* **2013**, *23*, 886–897. [[CrossRef](#)]
28. Li, W.; Khor, T.O.; Xu, C.; Shen, G.; Jeong, W.-S.; Yu, S.; Kong, A.-N. Activation of Nrf2-antioxidant signaling attenuates NFκB-inflammatory response and elicits apoptosis. *Biochem. Pharmacol.* **2008**, *76*, 1485–1489. [[CrossRef](#)]
29. Chen, H.; Fang, Y.; Li, W.; Orlando, R.C.; Shaheen, N.; Chen, X.L. NFκB and Nrf2 in esophageal epithelial barrier function. *Tissue Barriers* **2013**, *1*, e27463. [[CrossRef](#)]
30. Wakabayashi, N.; Slocum, S.L.; Skoko, J.J.; Shin, S.; Kensler, T.W. When NRF2 talks, who's listening? *Antioxid. Redox Signal.* **2010**, *13*, 1649–1663. [[CrossRef](#)]
31. Sivandzade, F.; Prasad, S.; Bhalerao, A.; Cucullo, L. NRF2 and NF-κB interplay in cerebrovascular and neurodegenerative disorders: Molecular mechanisms and possible therapeutic approaches. *Redox Biol.* **2019**, *21*, 101059. [[CrossRef](#)] [[PubMed](#)]
32. Haghani, A.; Cacciottolo, M.; Doty, K.R.; D'Agostino, C.; Thorwald, M.; Safi, N.; Levine, M.E.; Sioutas, C.; Town, T.C.; Forman, H.J.; et al. Mouse brain transcriptome responses to inhaled nanoparticulate matter differed by sex and APOE in Nrf2-Nfkb interactions. *eLife* **2020**, *9*, e54822. [[CrossRef](#)] [[PubMed](#)]
33. Liu, G.-H.; Qu, J.; Shen, X. NF-κB/p65 antagonizes Nrf2-ARE pathway by depriving CBP from Nrf2 and facilitating recruitment of HDAC3 to MafK. *Biochim. Biophys. Acta* **2008**, *1783*, 713–727. [[CrossRef](#)] [[PubMed](#)]
34. Zhang, H.; Zhou, L.; Yuen, J.; Birkner, N.; Leppert, V.; O'Day, P.A.; Forman, H.J. Delayed Nrf2-regulated antioxidant gene induction in response to silica nanoparticles. *Free Radic. Biol. Med.* **2017**, *108*, 311–319. [[CrossRef](#)]
35. Cummings, B.P.; Digitale, E.K.; Stanhope, K.L.; Graham, J.L.; Baskin, D.G.; Reed, B.J.; Sweet, I.R.; Griffen, S.C.; Havel, P.J. Development and characterization of a novel rat model of type 2 diabetes mellitus: The UC Davis type 2 diabetes mellitus UCD-T2DM rat. *Am. J. Physiol. Integr. Comp. Physiol.* **2008**, *295*, R1782–R1793. [[CrossRef](#)]
36. Kleinert, M.; Clemmensen, C.; Hofmann, S.; Moore, M.C.; Renner, S.; Woods, S.C.; Huypens, P.; Beckers, J.; de Angelis, M.H.; Schürmann, A.; et al. Animal models of obesity and diabetes mellitus. *Nat. Rev. Endocrinol.* **2018**, *14*, 140–162. [[CrossRef](#)]
37. Piccolo, B.D.; Graham, J.L.; Stanhope, K.L.; Fiehn, O.; Havel, P.J.; Adams, S.H. Plasma amino acid and metabolite signatures tracking diabetes progression in the UCD-T2DM rat model. *Am. J. Physiol. Metab.* **2016**, *310*, E958–E969. [[CrossRef](#)]
38. Piccolo, B.D.; Graham, J.L.; Stanhope, K.L.; Nookaew, I.; Mercer, K.E.; Chintapalli, S.V.; Wankhade, U.D.; Shankar, K.; Havel, P.J.; Adams, S.H.; et al. Diabetes-associated alterations in the cecal microbiome and metabolome are independent of diet or environment in the UC davis type 2 diabetes mellitus rat model. *Am. J. Physiol. Metab.* **2018**, *315*, E961–E972. [[CrossRef](#)]
39. Dimauro, I.; Pearson, T.; Caporossi, D.; Jackson, M.J. A simple protocol for the subcellular fractionation of skeletal muscle cells and tissue. *BMC Res. Notes* **2012**, *5*, 513. [[CrossRef](#)]
40. Thorwald, M.; Rodriguez, R.; Lee, A.; Martinez, B.; Peti-Peterdi, J.; Nakano, D.; Nishiyama, A.; Ortiz, R.M. Angiotensin receptor blockade improves cardiac mitochondrial activity in response to an acute glucose load in obese insulin resistant rats. *Redox Biol.* **2018**, *14*, 371–378. [[CrossRef](#)]
41. Thacker, J.S.; Yeung, D.H.; Staines, W.; Mielke, J.G. Total protein or high-abundance protein: Which offers the best loading control for Western blotting? *Anal. Biochem.* **2016**, *496*, 76–78. [[CrossRef](#)] [[PubMed](#)]
42. Kwak, S.K.; Kim, J.H. Statistical data preparation: Management of missing values and outliers. *Korean J. Anesthesiol.* **2017**, *70*, 407–411. [[CrossRef](#)] [[PubMed](#)]
43. Lanzillotta, A.; Sarnico, I.; Ingrassia, R.; Boroni, F.; Branca, C.; Benarese, M.; Faraco, G.; Blasi, F.; Chiarugi, A.; Spano, P.; et al. The acetylation of RelA in Lys310 dictates the NF-κB-dependent response in post-ischemic injury. *Cell Death Dis.* **2010**, *1*, e96. [[CrossRef](#)] [[PubMed](#)]
44. Giridharan, S.; Srinivasan, M. Mechanisms of NF-KB P65 and strategies for therapeutic manipulation. *J. Inflamm. Res.* **2018**, *11*, 407–419. [[CrossRef](#)]
45. Dong, J.; Jimi, E.; Zeiss, C.; Hayden, M.S.; Ghosh, S. Constitutively active NF-κB triggers systemic TNFα-dependent inflammation and localized TNFα-independent inflammatory disease. *Genes Dev.* **2010**, *24*, 1709–1717. [[CrossRef](#)]

46. Chen, F.; Haigh, S.; Barman, S.A.; Fulton, D.J.R. From form to function: The role of Nox4 in the cardiovascular system. *Front. Physiol.* **2012**, *3*, 412. [[CrossRef](#)]
47. Vázquez-Medina, J.P.; Popovich, I.; Thorwald, M.A.; Viscarra, J.A.; Rodriguez, R.; Sonanez-Organis, J.G.; Lam, L.; Peti-Peterdi, J.; Nakano, D.; Nishiyama, A.; et al. Angiotensin receptor-mediated oxidative stress is associated with impaired cardiac redox signaling and mitochondrial function in insulin-resistant rats. *Am. J. Physiol. Circ. Physiol.* **2013**, *305*, H599–H607. [[CrossRef](#)]
48. Asmat, U.; Abad, K.; Ismail, K. Diabetes mellitus and oxidative stress—A concise review. *Saudi Pharm. J.* **2015**, *24*, 547–553. [[CrossRef](#)]
49. Levy, S.; Forman, H.J. C-Myc is a Nrf2-interacting protein that negatively regulates phase II genes through their electrophile responsive elements. *IUBMB Life* **2010**, *62*, 237–246. [[CrossRef](#)]
50. Zhang, H.; Liu, H.; Davies, K.J.; Sioutas, C.; Finch, C.E.; Morgan, T.E.; Forman, H.J. Nrf2-regulated phase II enzymes are induced by chronic ambient nanoparticle exposure in young mice with age-related impairments. *Free Radic. Biol. Med.* **2012**, *52*, 2038–2046. [[CrossRef](#)]
51. Thorwald, M.A.; Godoy-Lugo, J.A.; Rodriguez, G.J.; Rodriguez, M.A.; Jamal, M.; Kinoshita, H.; Nakano, D.; Nishiyama, A.; Forman, H.J.; Ortiz, R.M. Nrf2-related gene expression is impaired during a glucose challenge in type II diabetic rat hearts. *Free Radic. Biol. Med.* **2019**, *130*, 306–317. [[CrossRef](#)] [[PubMed](#)]
52. Franklin, C.C.; Backos, D.S.; Mohar, I.; White, C.C.; Forman, H.J.; Kavanagh, T.J. Structure, function, and post-translational regulation of the catalytic and modifier subunits of glutamate cysteine ligase. *Mol. Asp. Med.* **2009**, *30*, 86–98. [[CrossRef](#)] [[PubMed](#)]
53. Li, M.-H.; Jang, J.-H.; Na, H.-K.; Cha, Y.-N.; Surh, Y.-J. Carbon monoxide produced by heme oxygenase-1 in response to nitrosative stress induces expression of glutamate-cysteine ligase in PC12 cells via activation of phosphatidylinositol 3-Kinase and Nrf2 signaling. *J. Biol. Chem.* **2007**, *282*, 28577–28586. [[CrossRef](#)] [[PubMed](#)]
54. Cherkas, A.; Holota, S.; Mdzinarashvili, T.; Gabbianelli, R.; Zarkovic, N. Glucose as a major antioxidant: When, what for and why it fails? *Antioxidants* **2020**, *9*, 140. [[CrossRef](#)]
55. Brand, M.D.; Affourtit, C.; Esteves, T.C.; Green, K.; Lambert, A.J.; Miwa, S.; Pakay, J.L.; Parker, N. Mitochondrial superoxide: Production, biological effects, and activation of uncoupling proteins. *Free Radic. Biol. Med.* **2004**, *37*, 755–767. [[CrossRef](#)]